Talanta 232 (2021) 122429

Contents lists available at ScienceDirect

Talanta

journal homepage: www.elsevier.com/locate/talanta

A highly sensitive method for simultaneous detection of hAAG and UDG activity based on multifunctional dsDNA probes mediated exponential rolling circle amplification

Longxing Fan [a,c,1], Wentao Liu [c,1], Boning Yang [c,1], Yingchun Zhang [b,c], Xiaotao Liu [a], Xinglin Wu [a,c], Baoan Ning [c], Yuan Peng [c], Jialei Bai [c,**], Liangqia Guo [a,*]

[a] Ministry of Education Key Laboratory for Analytical Science of Food Safety and Biology, Fujian Provincial Key Laboratory of Analysis and Detection Technology for Food Safety, College of Chemistry, Fuzhou University, Fuzhou, 350116, PR China
[b] Nankai University School of Medicine, Nan Kai University, 94 Weijin Road, Tianjin, 300071, PR China
[c] Tianjin Key Laboratory of Risk Assessment and Control Technology for Environment and Food Safety, Tianjin Institute of Environmental and Operational Medicine, Tianjin, 300050, PR China

ARTICLE INFO

Keywords:
Human alkyladenine DNA glycosylase
Uracil-DNA glycosylase
Biosensor
Fluorescence method
Exponential rolling circle amplification

ABSTRACT

DNA glycosylase is an indispensable DNA damage repair enzyme which can recognize and excise the damaged bases in the DNA base excision-repair pathway. The dysregulation of DNA glycosylase activity will give rise to the dysfunction of base excision-repair and lead to abnormalities and diseases. The simultaneous detection of multiple DNA glycosylases can help to fully understand the normal physiological functions of cells, and determine whether the cells are abnormal in pre-disease. Regrettably, the synchronous detection of functionally similar DNA glycosylases is a great challenge. Herein, we developed a multifunctional dsDNA probe mediated exponential rolling circle amplification (E-RCA) method for the simultaneously sensitive detection of human alkyladenine DNA glycosylase (hAAG) and uracil-DNA glycosylase (UDG). The multifunctional dsDNA probe contains the hypoxanthine sites and the uracil sites which can be recognized by hAAG and UDG respectively to generate apyrimidinic (AP) sites in the dsDNA probe. Then the AP sites will be recognized and cut by endonuclease IV (Endo IV) to release corresponding single-stranded primer probes. Subsequently, two padlock DNA templates are added to initiate E-RCA to generate multitudinous G-quadruplexes and/or double-stranded dumbbell lock structures, which can combine N-methyl mesoporphyrin IX (NMM) and SYBR Green I (SGI) for the generation of respective fluorescent signals. The detection limits are obtained as low as 0.0002 U mL^{-1} and 0.00001 U mL^{-1} for hAAG and UDG, respectively. Notably, this method can realize the simultaneous detection of two DNA glycosylases without the use of specially labeled probes. Finally, this method is successfully applied to detect hAAG and UDG activities in the lysates of HeLa cells and Endo1617 cells at single-cell level, and to detect the inhibitors of DNA glycosylases.

1. Introduction

Thousands of spontaneous DNA base lesions occur daily in living organisms. In order to counteract the harmful effects of DNA damage, there are various DNA repair mechanisms in organisms. Under normal circumstance, most DNA repair methods mainly rely on base excision-repair (BER) in the bodies [1–3]. The BER process is triggered by DNA glycosylases, which recognize the mismatched and anomalous bases, excise the damaged bases from gene by hydrolyzing the N-glycosidic bond between the base and deoxyribose, generate the AP sites, and eventually cooperate with other repair proteins to complete gene repair [4]. The abnormal level of DNA glycosylase in human cells is related to various diseases, such as cancers [5], cardiovascular diseases [6], nervous system diseases and some inflammation-related diseases [7,8].

* Corresponding author. Ministry of Education Key Laboratory of Analytical Science for Food Safety and Biology, Fujian Provincial Key Laboratory of Analysis and Detection Technology for Food Safety, College of Chemistry, Fuzhou University, Fuzhou, 350116, PR China.
** Corresponding author.
E-mail addresses: baijialeitj@163.com (J. Bai), lqguo@fzu.edu.cn (L. Guo).
[1] These three authors contributed equally to this work.

https://doi.org/10.1016/j.talanta.2021.122429
Received 19 February 2021; Received in revised form 9 April 2021; Accepted 10 April 2021
Available online 24 April 2021

Human alkyladenine DNA glycosylase (hAAG) and uracil-DNA glycosylase (UDG) play a vital role in protecting the integrity of the genome. hAAG is involved in cell cycle regulation, cell apoptosis [9] and various diseases, such as lung cancer [10] and cervical cancer [11]. Abnormal expression of UDG is associated with a variety of cancers, such as lung cancer [12], bowel cancer [13], and rectal cancer [14]. The development of sensitive and selective methods for the detection of multiple DNA glycosylases at the same time is essential for cancer biomedical research and clinical diagnosis.

Great efforts have been made for the detection of the DNA glycosylases and their activities. The traditional methods for the detection of DNA glycosylase mainly include high performance chromatography and mass spectrometry [15,16], gel electrophoresis analysis [17] and radioactive labeling [18], and so on. Although they can effectively detect DNA glycosylases, most of them are time-consuming, poor sensitivity or involving hazardous radiation, and can't detect the activities of DNA glycosylases. In order to simply and sensitively detect the activities of DNA glycosylases, a series of alternative methods have been developed, including polymerase chain reaction (PCR) [19], colorimetry [20], electrochemiluminescence [21,22], and fluorescence [23,24]. Among these methods, fluorescence technology has attracted much attention due to its simplicity, high sensitivity and good selectivity. Zhang's group has developed a new fluorescent method by two-tailed reverse transcription PCR and gold nanoparticle-mediated silver nanoclusters to measure the activity of UDG [25]. Jing's group reported a homogeneous sensitive fluorescent assay strategy to detect the activity of thymine DNA glycosylase (TDG) enzyme based on exonuclease-mediated signal amplification [26]. Ma's group developed a simple and convenient UDG detection method based on trivalent iridium ion complex as the G-quadruplexes recognition probe. In order to further improve the sensitivity, an amplification strategy was subsequently introduced to amplify the fluorescence signal [27]. Li's group proposed an exonuclease III mediated amplification strategy to detect the activity of human 8-oxoguanine DNA glycosylase 1 (hOGG1) [23]. Chen's group established a fluorescent method for the sensitive detection of hAAG based on Endo IV-mediated hyperbranched amplification. Usually there are abnormal expressions of multiple glycosylases in cancer cells, so the simultaneous detection of two or more DNA glycosylases can increase the reliability of cancer diagnosis. Today, the method for simultaneous recognition of multiple DNA glycosylases has seldomly been developed [28]. For example, Zhang's group developed a highly ingenious single-molecule detection strategy for simultaneous detection of hAAG and hOGG1 in lung cancer cells [10]. Tang and Zhang's team proposed an endonuclease Ⅳ-mediated amplification means to identify different types of glycosylases [29]. Unfortunately, there are few reports on the simultaneous detection of hAAG and UDG activities. Rolling circle amplification (RCA) is based on circular DNA, which can be started by a short DNA primer under constant temperature, and a large number of single-stranded DNA can be produced in a certain period of time. With the extension of reaction time, the products will prolong and become difficult to dissolve. In order to increase the solubility of the products, with the aid of restriction endonuclease, exponential rolling circle amplification (E-RCA) can produce a large number of dissolvable products with moderate length, thus further increasing the yield of amplification products.

In this work, we proposed a multifunctional dsDNA probe-mediated E-RCA method for highly sensitive detection of hAAG and UDG activities (Scheme 1). hAAG and UDG specifically recognized the hypoxanthine sites and uracil sites respectively to generate AP sites in dsDNA probes. Then the AP sites were cut by Endo Ⅳ to release respective primer probes. With the help of two padlock DNA (P-DNA) templates, the released primer probes trigger the E-RCA respectively to generate abundant G-quadruplexes and/or double-stranded dumbbell lock structures. NMM and SGI were used as the fluorescent dyes to specifically combine G-quadruplexes and double-stranded dumbbell lock structures, respectively. Therefore, the simultaneous detection of two

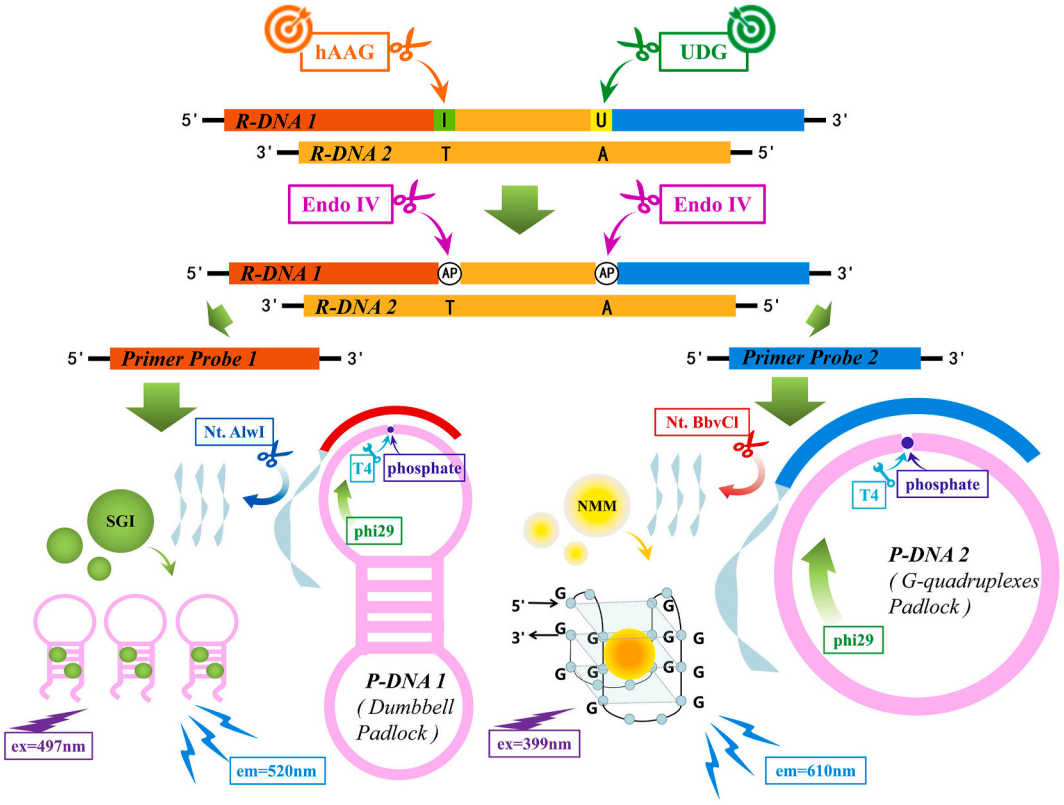

Scheme 1. Schematic illustration of the multifunctional dsDNA probes mediated exponential rolling circle amplification strategy for highly sensitive detection of hAAG and UDG activities.

DNA glycosylases was realized without the need to use special labeled probes. Finally, this method was applied for the detection of hAAG and UDG activities in the lysates of HeLa cells and Endo 1617 cells, and the inhibitors of DNA glycosylases.

2. Experimental section

2.1. Reagents and apparatus

DNA oligonucleotides were HPLC-purified and synthesized by Sangon Biotechnology Co. Ltd. (Shanghai, China). The sequences of DNA oligonucleotides were shown in Table S1. UDG, hAAG, foramidopyrimidine DNA glycosylase (Fpg), hOGG1, T4 DNA ligase (T4), Endo IV, Nt.BbvCI endonuclease (Nt.BbvCI), Nt.AlwI endonuclease (Nt.AlwI), deoxynucleotide triphosphates (dNTPs) and their buffers were purchased from New England Biolabs Ltd. (Beijing, China). phi29 polymerase (phi29) was purchased from Thermo (Beijing, China). 10,000 × SGI was obtained from Solarbio (Beijing, China). NMM was obtained from J&K Scientific Ltd.(Beijing, China). $CdCl_2$ was purchased from Sigma-Aldrich (Shanghai, China). All other reagents were of analytical reagent grade and were used without further purification. The solutions used in all experiments were prepared with Milli-Q water (18 MΩ cm). Fluorescence signal was recorded by a F97pro fluorescence spectrophotometer (Lengguang, China). DNA gels were imaged by an Amersham Imager 680 RGB (GE Healthcare, USA).

2.2. Procedures for the simultaneous detection of hAAG and UDG activities

The simultaneous detection of hAAG and UDG activities was operated at 37.0 °C and included two consecutive steps (Scheme 1). The first step is the recognition and cleavage of the mismatch sites in the dsDNA probe. The mixture containing R-DNA1 (1.0 μmol L^{-1}) and R-DNA2 (1.0 μmol L^{-1}) was incubated in PBS buffer (pH 7.2, 10 mmol L^{-1}) at 95.0 °C for 5 min and cooled to room temperature to form the dsDNA probes. 1 μL 10 × ThermoPol buffer was added to 5 μL above mixture, then different doses of hAAG and UDG were further added, and the volume of the mixture was expanded to 10 μL with Milli-Q water. The mixture was incubated for 1 h. Subsequently, 2 μL 10 × Endo IV buffer, 10 U Endo IV was added, and the volume of the mixture was expanded to 20 μL with Milli-Q water. The mixture was incubated for another 1 h to nick the dsDNA probe at the AP sites and release respective primer probes. The second step is signal amplification by E-RCA. 5 μL dumbbell padlock DNA (P-DNA1, 10 μmol L^{-1}), 5 μL G-quadruplex padlock DNA (P-DNA2, 10 μmol L^{-1}), 3 μL 10 × T4 DNA ligase buffer and 10 U T4 were added and reacted for 1 h, the volume of the mixture was expanded to more than 30 μL. After reaction, 5 μL dNTPs (1.0 μmol L^{-1}), 5 μL 10 × CutSmart buffer, 5 μL 10 × phi29 DNA polymerase buffer, 8 U Nt. BbvcI, 8 U Nt. A1wI and 10 U phi29 were added. The mixture was further expanded to 50 μL with Milli-Q water and incubated for 3 h. Finally, 20 μL KCl (1.0 mol L^{-1}), 8 μL NMM (50.0 μmol L^{-1}) and 20 μL SGI (in 10 × buffer solution) were added. And the mixture was expanded to 200 μL with Milli-Q water. After reaction for 30 min, the fluorescence spectra of the mixture solution were recorded at the excitation wavelength of 495 nm and 399 nm. The fluorescence intensities at 520 nm and 610 nm were used for quantitative detection of hAAG and UDG activities, respectively.

2.3. Gel electrophoresis analysis

The 12% polyacrylamide gel electrophoresis (PAGE) was employed to analyze the length and hybridization of DNA oligonucleotides and the activities of hAAG, UDG and Endo IV. The electrophoresis was carried out in 1 × TBE buffer at a constant voltage of 120 V for 50 min. The PAGE sample was stained with 1 × GenGreen solution buffer for 30 min. To verify and compare RCA and E-RCA, reaction products were analyzed by agarose gel electrophoresis. 1 × TAE buffer was used as a running buffer and a constant voltage of 80 V was applied on 2% (w/v) agarose gel for 1 h. Finally, all electrophoresis gels were imaged.

2.4. Cell culture and preparation of the cell lysates

The HeLa and Ende 1617 Cells were cultured in Dulbecco's modified Eagle's medium (DMEM) supplemented with 10% fetal bovine serum (FBS), and 1% penicillin/streptomycin at 37.0 °C in a humidified 5% CO_2 incubator. Approximately 1 × 10^6 cells were dispensed in a 1.5 mL centrifuge tube, washed twice with PBS buffer (pH 7.2, 10 mmol L^{-1}), and centrifuged at 100 g for 5 min and re-suspended in PBS buffer (pH 7.2, 10 mmol L^{-1}) by ultrasonication in 4.0 °C. After the cell lysis solution was centrifuged to discard cell debris at 10,000 g for 10 min at 4.0 °C. The supernatant was filtered by a 0.45 μm filter membrane and stored at 4.0 °C. Finally, the cell lysis solution was diluted with PBS buffer (pH 7.2, 10 mmol L^{-1}), and the final concentration of the cell lysate for detection was equivalent to 1 × 10^0, 1 × 10^1, 1 × 10^2, and 1 × 10^3 cells.

2.5. Assays of inhibitor

To evaluate the inhibition of hAAG and UDG activity, $CdCl_2$ was selected as the model inhibitor. Different concentrations of $CdCl_2$ solution with 10 U hAAG or UDG was incubated at 37.0 °C for 20 min, and then the following operations were the same with the procedures for the detection of hAAG and UDG activities. The IC_{50} value of inhibitor was analyzed using IBM SPSS statistics 22.0 software.

3. Results and discussion

3.1. The principle of this strategy

The principle for the detection of hAAG and UDG activities was shown in Scheme 1. R-DNA1 and R-DNA2 were mixed and hybridized to prepare multifunctional dsDNA probes. The sequence of R-DNA1 in the dsDNA probe contains a hypoxanthine site (in green "I") and a uracil (in yellow "U") site. R-DNA2 plays a role in assisting glycosylase recognition. hAAG and UDG could recognize the hypoxanthine and uracil sites, respectively and remove the mismatch bases to form the AP sites, which could be recognized and nicked by Endo IV to release respective primer probe from the dsDNA probes. Hereafter, the specific primer probes (primer probe 1 and/or primer probe 2) would trigger E-RCA with the help of two padlock DNA (P-DNA) templates and enzymes including T4, phi29, Nt.BbvCI or NT. A1wI, and finally produced multitudinous G-quadruplexes and/or double-stranded dumbbell lock structures. SGI and NMM could combine to the double-stranded dumbbell lock structures and G-quadruplexes respectively to generate "turn-on" fluorescent signals, which represented the activities of hAAG and UDG, respectively.

3.2. Feasibility of this method

In order to investigate the feasibility of this method, PAGE electrophoresis was performed using GenGreen as the fluorescent indicator to explore the hydrolysis products. In Fig. 1A, lanes 1, 2, and 3 showed the smears of R-DNA1, R-DNA2 and the dsDNA probe, respectively. Only in the presence of hAAG, the smear of the dsDNA probe was not changed (Lane 4). The presence of low molecular weight band in Lane 5 indicated the dsDNA probe was nicked at the AP sites to release primer probe 1 in the presence of both hAAG and Endo IV. Similar phenomena were observed for UDG in Lanes 6–7 The reduction of dsDNA probe band and the emergence of multiple low molecular weight bands in Lane 8 indicated the release of primer probe 1 and 2 from the dsDNA probe in the simultaneous presence of hAAG, UDG and Endo IV. These results confirmed that hAAG and UDG could recognize the "I" and "U" sites respectively in the dsDNA probes, and the products (primer probe 1 and/

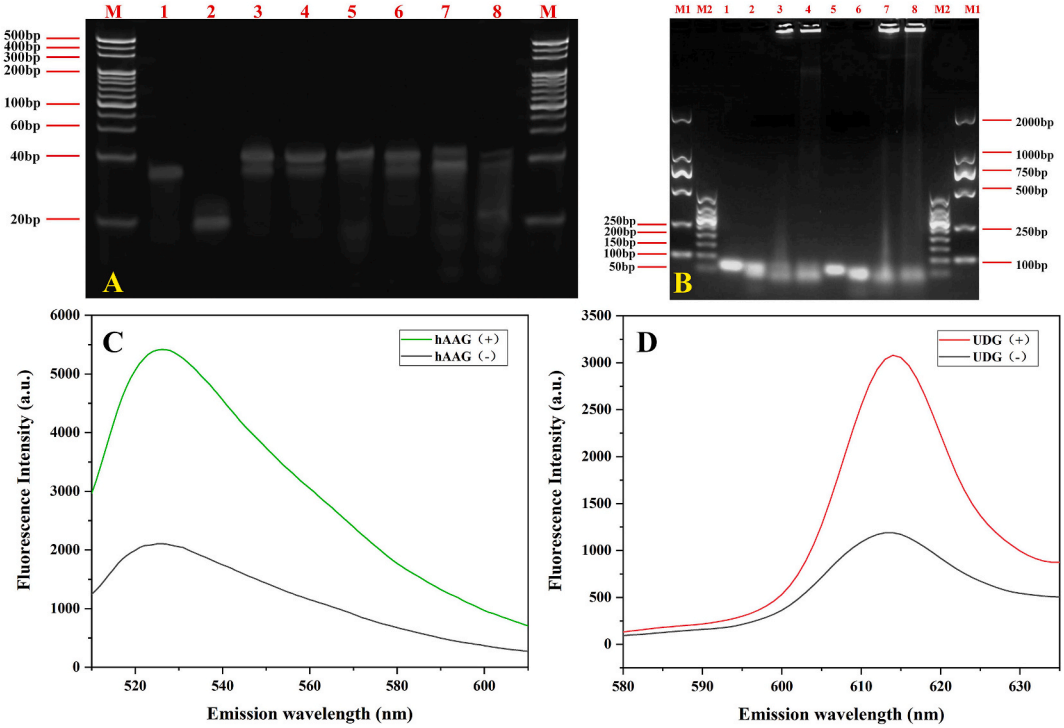

Fig. 1. (A) Polyacrylamide gel electrophoresis analysis of the activities of hAAG, UDG and Endo IV acting on the dsDNA probeduplex (Lane M: DNA size marker, Lane 1: R-DNA1, Lane 2: R-DNA2, Lane 3: R-DNA1+R-DNA2 (dsDNA), Lane 4: dsDNA + hAAG, Lane 5: dsDNA + hAAG + EndoIV, Lane 6: dsDNA + UDG, Lane 7: dsDNA + UDG + EndoIV, Lane 8: dsDNA + hAAG + UDG + EndoIV). (B) Agarose gel electrophoresis analysis of the amplification products of the dumbbell padlock probe trigger by hAAG and the amplification of the UDG trigger padlock probe (Lane M1 and M2: DNA size markers, Lane 1: P-DNA1, Lane 2: P-DNA1 + dsDNA + hAAG + EndoIV + T4, Lane 3: P-DNA1 + dsDNA + hAAG + EndoIV + T4 + phi29, Lane 4: P-DNA2 + dsDNA + hAAG + EndoIV + T4 + phi29 + Nt.AlwI, Lane 5: P-DNA2, Lane 6: P-DNA2 + dsDNA + UDG + EndoIV + T4, Lane 7: P-DNA2 + dsDNA + UDG + EndoIV + T4 + phi29, Lane 8: P-DNA2 + dsDNA + UDG + EndoIV + T4 + phi29 + Nt.BbvCI). Typical fluorescent emission spectra of the system in the presence or absence of hAAG (C) and UDG (D).

or primer probe 2) could be produced and released with the help of Endo IV. Agarose gel electrophoresis experiments were further performed to verify the amplified products (Fig. 1B). Lanes 1–4 were designed to verify E-RCA of dumbbell-locked DNA template in the presence of hAAG. Lane 1 showed the smear of P-DNA1. Lane 2 indicated the mixture of P-DNA1 and the product of dsDNA probe after interaction with hAAG and Endo IV. Because of the absence of phi29, dumbbell lock probe amplification template could not be formed; there was no initiator of E-RCA. In the presence of the dumbbell lock template, amplification products of the RCA reaction were observed (Fig. 1B, lane 3). Line 4 represented the amplification products of the E-RCA reaction, indicating that the amplified product could be cleaved by Nt. A1wI to form a double-stranded structure. Lanes 5–8 were designed to verify E-RCA of padlock DNA probe in the presence of UDG. Lane 5 showed the smear of P-DNA2. Lane 6 indicated the mixture of P-DNA2 and the product of dsDNA probe after interaction with UDG and Endo IV. In the presence of the padlock template, amplification products of the RCA reaction were observed (Fig. 1B, lane 7). Line 8 represented the amplification products of the E-RCA reaction, indicating that the amplified product can be cleaved by Nt.BbvCI to form a G-quadruplex structure. The products of E-RCA and RCA were significantly different. Due to the action of restriction endonucleases, the products of E-RCA could be sliced into different lengths of single-stranded DNAs. The products of E-RCA (lanes 4 and 8) showed uniform smears in the lanes over the whole molecular range after dyeing. While the products of RCA (lanes 3 and 7) were uneven, either they were very long or short, that showed uneven tailing of smears (The comet tail smears were in the lower end of lanes) without the action of restriction endonucleases. When restriction endonucleases were present, the products could be hydrolyzed to form DNA fragments of different lengths, which facilitated its uniform dispersion and improved amplification efficiency in the solution. Obviously, compared to RCA, E-RCA could produce more soluble DNA fragments, thereby producing a higher and more stable fluorescence signal. Furthermore, the fluorescence intensities of the system were enhanced in the presence of hAAG (Fig. 1C) and UDG (Fig. 1D), which provided the possibility for the quantitative detection of hAAG and UDG activities.

3.3. Optimization of experimental conditions

The length of R-DNA2 played a key regulatory role in the release of primer probes. Therefore, the length of R-DNA2 was optimized. As shown in Fig. 2, the length of R-DNA2-0 was optimized at 30 nt by taking account of high fluorescent intensities for both hAAG and UDG. Therefore, 30 nt length R-DNA2 was selected for subsequent experiments.

The activities of Endo IV, T4, phi29, Nt. A1wI and Nt.BbvCI, the concentration of SYBR-Green I and NMM, and the reaction time for fluorescence evolution were also optimized. According to the controlled variable method, the experimental conditions were investigated to improve the relative fluorescence intensity ($\triangle$F) of the system in the presence and absence of glycosylase. And the results were shown in Figs. S1–S8. It was found in Fig. S1 that the $\triangle$F reached a platform when Endo IV activity exceeded 10 U, which meat that 10 U Endo IV was sufficient to nick the AP sites. The dosage of T4 and phi29 were also critical to the E-RCA. As shown in Figs. S2 and S3, when the activity of T4 reached 8 U and the activity of phi29 reached 10 U, the $\triangle$F reached a plateau. Therefore 8 U T4 and 10 U phi29 were selected for subsequent experiments. The E-RCA reaction was also closely related to the activities of Nt. A1wI and Nt.BbvCI. Figs. S4 and S5 showed that the activities of Nt. A1wI and Nt.BbvCI were optimized both at 8 U. The concentration of fluorescent dye was critical to the fluorescence signal. 20 μL 10 × SGI solution (Fig. S6) and 2 μmol L^{-1} NMM solution (Fig. S7) were selected for subsequent experiments. The fluorescence intensity was gradually

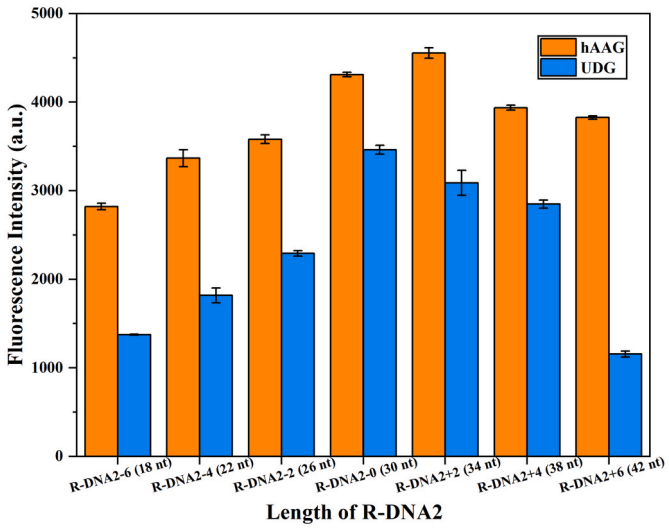

Fig. 2. Effect of the length of R-DNA2 on the fluorescence intensities for the detection of hAAG and UDG activities. Error bars show the standard deviations of the results from three independent experiments.

enhanced with the increasing of reaction time and reached a plateau after 3 h. Therefore, 3 h was selected as the optimal reaction time for subsequent experiments.

3.4. Sensitivity of this method

Under the optimized conditions, the sensitivity of this method was studied by measuring the fluorescence intensity in the presence of different concentrations of glycosylase. As shown in Fig. 3A, the fluorescence intensity was gradually increased with the increasing of hAAG concentration from 0.0001 to 20 U mL^{-1}. When the maximal fluorescence intensity of the system in the presence of 20 U mL^{-1} hAAG was normalized to 1, there was a good linear relationship between the normalized fluorescence intensity (F) and hAAG concentration (C) over the concentration range of 0.0005–20 U mL^{-1} (Fig. 3B). The linear relationship could be expressed as $F = 0.7154 + 0.1867 \log_{10} C$ ($R^2 = 0.9979$). The detection limit for hAAG activity was 0.0002 U mL^{-1} according to the 3δ rule. The fluorescence signals with the increasing concentrations of UDG were shown in Fig. 3C. There was a good linear relationship between the normalized fluorescence intensity (F) and UDG concentration (C) over the concentration range of 0.0001–20 U mL^{-1} (Fig. 3D). The linear relationship could be expressed as $F = 0.7676 + 0.1765 \log_{10} C$ ($R^2 = 0.9972$). The detection limit for UDG activity was 0.00001 U mL^{-1} according to the 3δ rule. Compared with the previously reported fluorescent methods for hAAG [28] and UDG [30], this method exhibited a wider linear range and lower detection limit (Table S2) [31–33,35–37].

3.5. Selectivity of this method

The selectivity of this method mainly relied on the specific recognition of hAAG to the hypoxanthine base and UDG to the uracil base. To evaluate the selectivity of this method, the analogs Fpg and hOGG1 were chosen as the interference factors. As shown in Fig. 4A, only hAAG

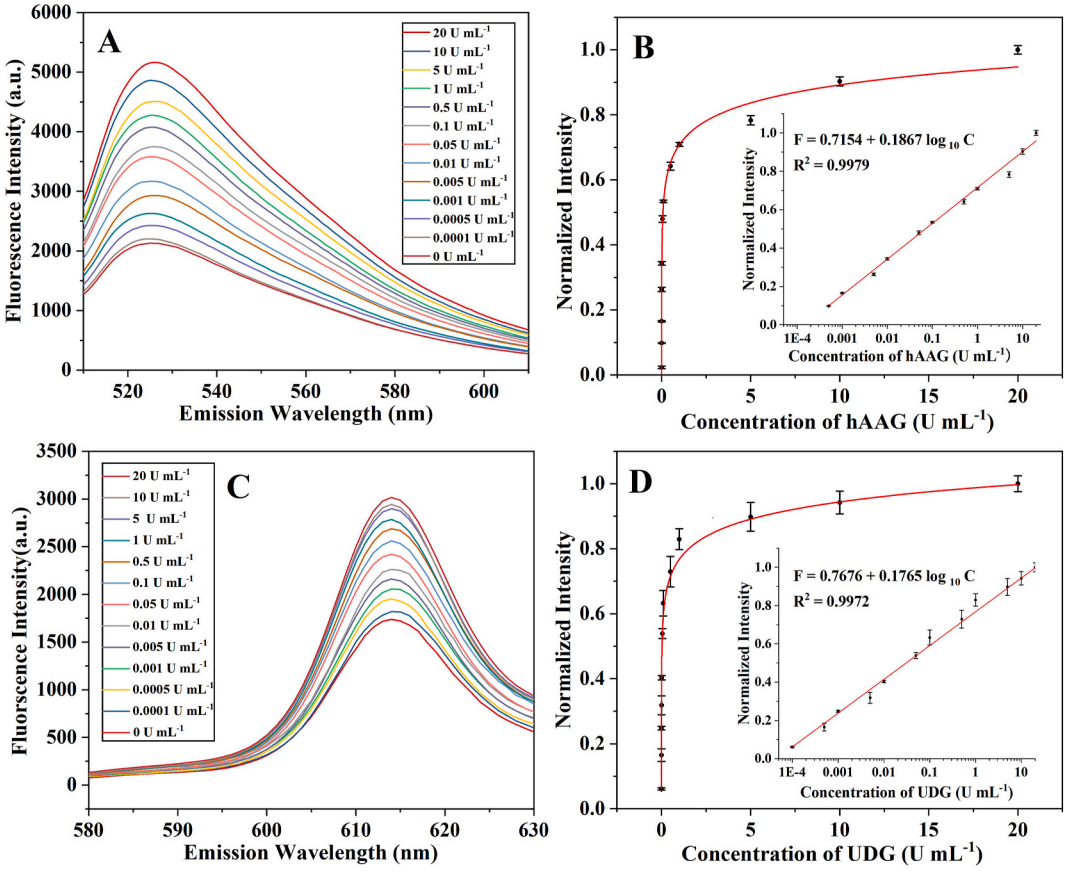

Fig. 3. Fluorescence emission spectra in the presence of different concentrations of hAAG (A) and UDG (C). The response curve of the normalized intensity in the presence of different concentration of hAAG (B) and UDG (D). Inset: the linear relationship between the normalized intensity and hAAG (B) and UDG (D) concentration, respectively. Error bars represent the standard deviations for three independent experiments.

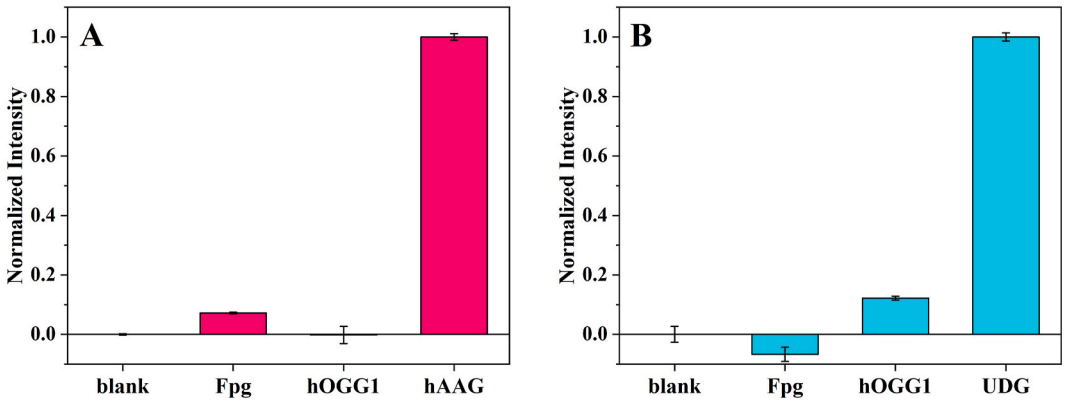

Fig. 4. (A) Specificity of hAAG activity assay. (B) Specificity of UDG activity assay. Error bars represented the standard deviations of the results from three independent experiments. The amount of the target enzymes or the non-target enzymes used was 10 U.

caused a high fluorescence signal, and the fluorescence intensities of other enzymes were almost the same as that of the blank. Similarly, Fig. 4B showed that the fluorescence signal was not significantly enhanced except UDG, but hOGG1 may slightly interfere in the detection of UDG. These results indicated that this method exhibited good selectivity for hAAG and UDG.

3.6. Detection of hAAG and UDG activities in cell lysates

In order to verify the practical applicability and reliability of this method, hAAG and UDG activities in the lysates of HeLa and Ende1617 cells were detected. As shown in Fig. 5A and B, the fluorescence intensities were increased with the increasing quantity of HeLa and Ende1617 cells. The fluorescence intensities were normalized to that of the normal cells (Ende1617) in the order of 10°, which is helpful for evaluating the expression of hAAG and UDG in different types of cells. All the original data were statistically analyzed by SPSS22.0 software. The analysis of variance (ANOVA) of hAAG and UDG of HeLa and Ende1617 showed that the expression of enzyme increased with the increase of the number of cells. The hAAG and UDG of HeLa and Ende1617 in different groups were tested by T test, and it was found that there were significant statistical differences among all groups ($P < 0.05$). It was found that the activity of hAAG in cancer cells was slightly higher than that in normal cells, while the activity of UDG in tumor cells was significantly higher than that in normal cells. This result indicated that there were lots of DNA damage or mismatches in tumor cells, and the BER was initiated, so that the expression of two DNA glycosylases was up-regulated [38]. Thus, this method can achieve the detection of DNA glycosylase concentration at single-cell level and evaluate the activities of different DNA glycosylases in different types of cells. This result was consistent to previous reports [39,40].

3.7. Detection of the inhibitor of hAAG and UDG activity

In order to evaluate the feasibility of this method for inhibitor detection, Cd^{2+} was selected as a model inhibitor of DNA glycosylase. As shown in Fig. 6 that the relative fluorescence intensities were gradually decreased with the increasing concentration of Cd^{2+}, indicating that the activities of hAAG and UDG were gradually inhibited. The IC_{50} value was selected to evaluate the inhibitory effect of Cd^{2+} on the activities of hAAG and UDG. As shown in Fig. 6, the IC_{50} values of Cd^{2+} to hAAG and UDG were calculated to be 41.53 μM and 48.65 μM, respectively, which was similar with previous reports by fluorescence methods [10,34]. Therefore, this method might provide a new platform for the screening of DNA glycosylase inhibitors.

4. Conclusions

In summary, a multifunctional dsDNA probe mediated E-RCA method for the simultaneously sensitive detection of hAAG and UDG were developed in a homogeneous reaction. The detection limits for hAAG and UDG were achieved at 0.0002 U mL^{-1} and 0.00001 U mL^{-1}, respectively. This method has been successfully applied to detect the activity of hAAG and UDG in real complex cell samples and the inhibitors of hAAG and UDG. It is expected that the method can be extended to detect other DNA glycosylases by replacing the specific base

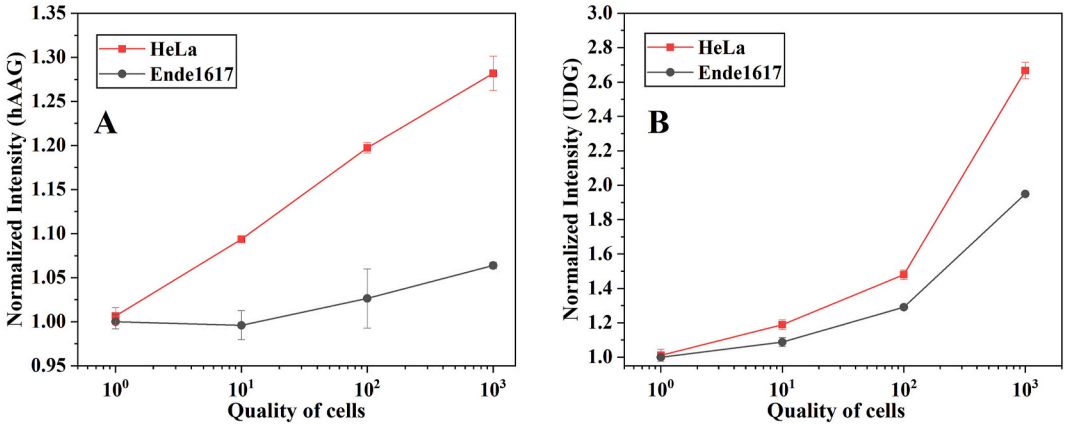

Fig. 5. (A) Detection of hAAG activity in the lysates of HeLa and Ende1617 cells. (B) Detection of UDG activity in the lysates of HeLa and Ende1617 cells. Error bars represented the standard deviations for three independent experiments.

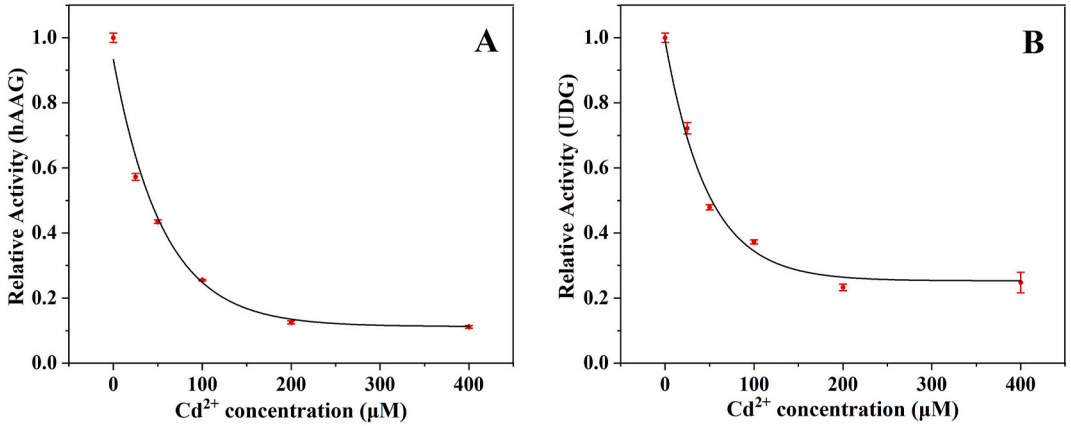

Fig. 6. (A) Detection of the relative activity of 10U hAAG in response to different Cd^{2+} concentrations. (B) Detection of the relative activity of 10U UDG in response to different Cd^{2+} concentrations. Error bars were calculated from three replicate measurements.

in the substrate of dsDNA probe, and has great potential in biomedical research and diagnosis.

Credit author statement

Longxing Fan: Conceptualization, Methodology, Formal analysis, Writing – original draft. **Wentao Liu**: Software, Formal analysis, Writing – original draft. **Boning Yang**: Formal analysis, Writing – original draft. **Yingchun Zhang**: Validation, Investigation. **Xiaotao Liu**: Validation, Investigation. **Xinglin Wu**: Validation, Investigation. **Baoan Ning**: Resources, Supervision, Project administration. **Yuan Peng**: Resources, Funding acquisition. **Jialei Bai**: Resources, Writing – review & editing. **Liangqia Guo**: Writing – review & editing, Supervision

Declaration of competing interest

The authors declare that they have no known competing financial interests or personal relationships that could have appeared to influence the work reported in this paper.

Acknowledgements

This work was supported by the National Key Research and Development Program of China (No. 2018YFC1602600), the National Natural Science Foundation of China (No. 21976210; 2019CXTD03) and the Natural Science Foundation of Inner Mongolia (No. 2019MS08026).

Appendix A. Supplementary data

Supplementary data to this article can be found online at https://doi.org/10.1016/j.talanta.2021.122429.

References

[1] R.J. Carter, J.L. Parsons, Base excision repair, a pathway regulated by posttranslational modifications, Mol. Cell Biol. 36 (2006) 1426–1437, https://doi.org/10.1128/mcb.00030-16.
[2] G.T. Sáez, DNA injury and repair systems, Int. J. Mol. Sci. 19 (2018) 1902–1904, https://doi.org/10.3390/ijms19071902.
[3] G.N. Wogan, S.S. Hecht, J.S. Felton, A.H. Conney, L.A. Loeb, Environmental and chemical carcinogenesis, Semin. Canc. Biol. 14 (2004) 473–486, https://doi.org/10.1016/j.semcancer.2004.06.010.
[4] Y.J. Kim, D.M. Wilson, Overview of base excision repair biochemistry, Curr. Mol. Pharmacol. 5 (2012) 3–13, https://doi.org/10.2174/1874467211205010003.
[5] G. Jie, X. Gao, J. Ge, C. Li, Multifunctional DNA nanocage with CdTe quantum dots for fluorescence detection of human 8-oxoG DNA glycosylase 1 and doxorubicin delivery to cancer cells, Microchim. Acta 186 (2019) 85, https://doi.org/10.1007/s00604-018-3199-2.
[6] Y. Liu, L.Y. Sun, D.V. Singer, R. Ginnan, W. Zhao, F.L. Jourd'heuil, D. Jourd'heuil, X. Long, H.A. Singer, Thymine DNA glycosylase is a key regulator of CaMKIIγ expression and vascular smooth muscle phenotype, Am. J. Physiol. Heart Circ. Physiol. 317 (2019) H969–H980, https://doi.org/10.1152/ajpheart.00146.2019.
[7] X. Ba, L. Aguilera-Aguirre, Q.T. Rashid, A. Bacsi, Z. Radak, S. Sur, K. Hosoki, M. L. Hegde, I. Boldogh, The role of 8-oxoguanine DNA glycosylase-1 in inflammation, Int. J. Mol. Sci. 15 (2014) 16975–16997, https://doi.org/10.3390/ijms150916975.
[8] D.K. Jeppesen, V.A. Bohr, T. Stevnsner, DNA repair deficiency in neurodegeneration, Prog. Neurobiol. 94 (2011) (2011) 166–200, https://doi.org/10.1016/j.pneurobio.2011.04.013.
[9] G.E. Kisby, H. Lesselroth, A. Olivas, L. Samson, B. Gold, K. Tanaka, M.S. Turker, Role of nucleotide- and base-excision repair in genotoxin-induced neuronal cell death, DNA Repair 3 (2004) 617–627, https://doi.org/10.1016/j.dnarep.2004.02.005.
[10] J. Hu, M.H. Liu, Y. Li, B. Tang, C.Y. Zhang, Simultaneous sensitive detection of multiple DNA glycosylases from lung cancer cells at the single-molecule level, Chem. Sci. 9 (2018) 712–720, https://doi.org/10.1039/c7sc04296e.
[11] G. Gines, C. Saint-Pierre, D. Gasparutto, On-bead fluorescent DNA nanoprobes to analyze base excision repair activities, Anal. Chim. Acta 812 (2014) 168–175, https://doi.org/10.1016/j.aca.2013.12.038.
[12] L.D. Weeks, P. Fu, S.L. Gerson, Uracil-DNA glycosylase expression determines human lung cancer cell sensitivity to pemetrexed, Mol. Canc. Therapeut. 12 (2013) 2248–2260, https://doi.org/10.1158/1535-7163.mct-13-0172.
[13] C. Dusseau, G.I. Murray, R.A. Keenan, T. O'Kelly, H.E. Krokan, H.L. McLeod, Analysis of uracil DNA glycosylase in human colorectal cancer, Int. J. Oncol. 18 (2001) 393–399, https://doi.org/10.3892/ijo.18.2.393.
[14] M. Serizawa, T. Yokota, A. Hosokawa, K. Kusafuka, T. Sugiyama, Y. Tsubosa, H. Yasui, T. Nakajima, Y. Koh, The efficacy of uracil DNA glycosylase pretreatment in amplicon-based massively parallel sequencing with DNA extracted from archived formalin-fixed paraffin-embedded esophageal cancer tissues, Cancer Genet 208 (2015) 415–427, https://doi.org/10.1016/j.cancergen.2015.05.001.
[15] A. Darwanto, A. Farrel, D.K. Rogstad, L.C. Sowers, Characterization of DNA glycosylase activity by matrix-assisted laser desorption/ionization time-of-flight mass spectrometry, Anal. Biochem. 394 (2009) 13–23, https://doi.org/10.1016/j.ab.2009.07.015.
[16] D. Gackowski, E. Speina, M. Zielinska, J. Kowalewski, R. Rozalski, A. Siomek, T. Paciorek, B. Tudek, R. Olinski, Products of oxidative DNA damage and repair as possible biomarkers of susceptibility to lung cancer, Canc. Res. 63 (2003) 4899–4902, https://doi.org/10.1002/cncr.11601.
[17] G.L. Dianov, Monitoring base excision repair by in vitro assays, Toxicology 193 (2003) 35–41, https://doi.org/10.1016/S0300-483X(03)00288-9.
[18] E.L. Kreklau, M. Limp-Foster, N. Liu, Y. Xu, M.R. Kelley, L.C. Erickson, A novel fluorometric oligonucleotide assay to measure O (6)-methylguanine DNA methyltransferase, methylpurine DNA glycosylase, 8-oxoguanine DNA glycosylase and abasic endonuclease activities: DNA repair status in human breast carcinoma cells overexpressing methylpurine DNA glycosylase, Nucleic Acids Res. 29 (2001) 2558–2566, https://doi.org/10.1093/nar/29.12.2558.
[19] Y. Feng, S. Cai, G. Xiong, G. Zhang, S. Wang, X. Su, C. Yu, Sensitive detection of DNA lesions by bulge-enhanced highly specific coamplification at lower denaturation temperature polymerase chain reaction, Anal. Chem. 89 (2017) 8084–8091, https://doi.org/10.1021/acs.analchem.7b01599.
[20] Z. Wu, Z.K. Wu, H. Tang, L.J. Tang, J.H. Jiang, Activity-based DNA-gold nanoparticle probe as colorimetric biosensor for DNA methyltransferase/glycosylase assay, Anal. Chem. 85 (2013) 4376–4383, https://doi.org/10.1471/ac3o3575f.
[21] Y. Wu, X. Yang, B. Zhang, L.H. Guo, An electrochemiluminescence biosensor for 8-oxo-7,8-dihydro-2'-deoxyguanosine quantification and DNA repair enzyme activity analysis using a novel bifunctional probe, Biosens. Bioelectron. 69 (2015) 235–240, https://doi.org/10.1016/j.bios.2015.02.037.
[22] Z. Guo, B. Qiao, Q. Guo, H. Zhang, C. Cai, J.J. Feng, Dual-signal ratiometric electrochemiluminescence assay for detecting the activity of human methyltransferase, Analyst 143 (2018) 3353–3359, https://doi.org/10.1039/c8an00611c.

[23] X. Wang, T. Hou, T. Lu, F. Li, Autonomous exonuclease III-assisted isothermal cycling signal amplification: a facile and highly sensitive fluorescence DNA glycosylase activity assay, Anal. Chem. 86 (2014) 9626–9631, https://doi.org/10.1021/ac502125z.

[24] Y. Wu, L. Wang, W. Jiang, Toehold-mediated strand displacement reaction-dependent fluorescent strategy for sensitive detection of uracil-DNA glycosylase activity, Biosens. Bioelectron. 89 (2017) 984–988, https://doi.org/10.1016/j.bios.2016.10.053.

[25] K. Zhang, W. Huang, Y. Huang, K. Wang, X. Zhu, M. Xie, Determination of the activity of uracil-DNA glycosylase by using two-tailed reverse transcription PCR and gold nanoparticle-mediated silver nanocluster fluorescence: a new method for gene therapy-related enzyme detection, Microchim. Acta. 186 (2019) 181, https://doi.org/10.1007/s00604-019-3307-y.

[26] C. Chen, D. Zhou, H. Tang, M. Liang, J. Jiang, A sensitive, homogeneous fluorescence assay for detection of thymine DNA glycosylase activity based on exonuclease-mediated amplification, Chem. Commun. 49 (2013) 5874–5876, https://doi.org/10.1039/c3cc41700j.

[27] S. Lin, L. Lu, T.S. Kang, C. Liu, J.L. Mergny, C.H. Leung, D.L. Ma, Interaction of an iridium(iii) complex with g-quadruplex dna and its application in luminescent switch-on detection of siglec-5, Anal. Chem. 88 (2016) 10290–10295, https://doi.org/10.1021/acs.analchem.6b03128.

[28] L. Wang, H. Zhang, Y. Xie, H. Chen, C. Ren, X. Chen, Target-mediated hyperbranched amplification for sensitive detection of human alkyladenine DNA glycosylase from HeLa cells, Talanta 194 (2019) 846–851, https://doi.org/10.1016/j.talanta.2018.10.083.

[29] C.C. Li, Y. Zhang, B. Tang, C.Y. Zhang, Integration of single-molecule detection with magnetic separation for multiplexed detection of DNA glycosylases, Chem. Commun. 54 (2018) 5839–5842, https://doi.org/10.1039/C8CC01695J.

[30] X. Xu, L. Wang, Y. Wu, W. Jiang, Uracil removal-inhibited ligase reaction in combination with catalytic hairpin assembly for the sensitive and specific detection of uracil-DNA glycosylase activity, Analyst 142 (2017) 4655–4660, https://doi.org/10.1039/c7an01666b.

[31] H. Zhang, L. Wang, Y. Xie, X. Zuo, H. Chen, X. Chen, Base excision repair mediated cascading triple-signal amplification for the sensitive detection of human alkyladenine DNA glycosylase, Analyst 144 (2019) 3064–3071, https://doi.org/10.1039/c9an00200f.

[32] L.J. Wang, M.L. Luo, X.Y. Yang, X.F. Li, Y. Wu, C.Y. Zhang, Controllable autocatalytic cleavage-mediated fluorescence recovery for homogeneous sensing of alkyladenine DNA glycosylase from human cancer cells, Theranostics 9 (2019) 4450–4460, https://doi.org/10.7150/thno.35393.

[33] C.C. Li, W.X. Liu, J. Hu, C.Y. Zhang, A single quantum dot-based nanosensor with multilayer of multiple acceptors for ultrasensitive detection of human alkyladenine DNA glycosylase, Chem. Sci. 10 (2019) 8675–8684, https://doi.org/10.1021/ac9026675.

[34] G. Liu, W. He, C. Liu, Sensitive detection of uracil-DNA glycosylase (UDG) activity based on terminal deoxynucleotidyl transferase-assisted formation of fluorescent copper nanoclusters (CuNCs), Talanta 195 (2019) 320–326, https://doi.org/10.1016/j.talanta.2018.11.083.

[35] X. Chen, Y. Wu, G. Cao, X. Wang, Z. Ji, D. Huo, F. Xu, C. Hou, A methodology for ultrasensitive detection of sequence-specific DNA or uracil-DNA glycosylase activity, ACS Sens. 5 (2020) 1615–1623, https://doi.org/10.1021/acssensors.0c00081.

[36] F. Yang, X. Li, J. Li, Y. Xiang, R. Yuan, Target-triggered activation of rolling circle amplification for label-free and sensitive fluorescent uracil-DNA glycosylase activity detection and inhibition, Talanta 204 (2019) 812–816, https://doi.org/10.1016/j.talanta.2019.06.065.

[37] C.C. Li, H.Y. Chen, J. Hu, C.Y. Zhang, Rolling circle amplification-driven encoding of different fluorescent molecules for simultaneous detection of multiple DNA repair enzymes at the single-molecule level, Chem. Sci. 11 (2020) 5724–5734, https://doi.org/10.1039/D0SC01652G.

[38] S.S. Wallace, D.L. Murphy, J.B. Sweasy, Base excision repair and cancer, Canc. Lett. 327 (2012) 73–89, https://doi.org/10.1016/j.canlet.2011.12.038.

[39] L. Fan, Y. Peng, B. Ning, H. Wei, Z. Gao, J. Bai, L. Guo, A tri-functional probe mediated exponential amplification strategy for highly sensitive detection of Dnmt1 and UDG activities at single-cell level, Anal. Chim. Acta 1103 (2020) 164–173, https://doi.org/10.1016/j.aca.2019.12.058.

[40] L.J. Wang, M. Ren, Q. Zhang, B. Tang, C.Y. Zhang, Excision repair-initiated enzyme-assisted bicyclic cascade signal amplification for ultrasensitive detection of uracil-dna glycosylase, Anal. Chim. 89 (2017) 4488–4494, https://doi.org/10.1021/acs.analchem.6b04673.